

# Connection between extraordinary transmission and negative refraction in a prism of stacked sub-wavelength hole arrays

M Beruete<sup>1</sup>, M Navarro-Cía<sup>1</sup>, F Falcone<sup>1</sup>, I Campillo<sup>2</sup> and M Sorolla<sup>1</sup>

<sup>1</sup> Millimetre and Terahertz Waves Laboratory, Universidad Pública de Navarra, 31006 Pamplona, Spain

<sup>2</sup> CIC nanoGUNE Consolider, Tolosa Hiribidea 76, 20018 Donostia, Spain

E-mail: [mario@unavarra.es](mailto:mario@unavarra.es)

Received 17 March 2009, in final form 11 June 2009

Published 31 July 2009

Online at [stacks.iop.org/JPhysD/42/165504](http://stacks.iop.org/JPhysD/42/165504)

## Abstract

A prism engineered by stacking sub-wavelength hole arrays is shown as a route to negative refraction in any frequency range. We analyse numerically and experimentally at the near field zone, several propagation regimes and bands with orthogonal polarizations, and find that negative refraction is intimately linked to the extraordinary transmission resonance of sub-wavelength hole arrays. Negative indices of refraction start from near to zero values for the lower mode while for the second one they are positive. The p-polarization component has a positive refractive index within both bands. The way to engineering negative refraction devices in any region of the spectrum is open.

(Some figures in this article are in colour only in the electronic version)

## 1. Introduction

One of the challenges of today's metamaterials exhibiting negative refractive index (NRI) is having low losses, particularly at the optical part of the spectrum [1]. This is essential for designing perfect lenses [2], a concept that arose after the first experimental confirmation of NRI by using a prism made of metallic wires and split rings resonators working at microwave frequencies [3]. All these results have been derived following the seminal predictions made by Veselago in the late 1960s of the last century [4], where he theorized about the consequences of media simultaneously exhibiting negative permittivity and permeability. This makes possible a NRI which produces the inversion of Snell's refraction law at the interface between a standard and a NRI medium.

The phenomenon of negative refraction was demonstrated initially in dielectric photonic crystals, i.e. in inhomogeneous periodic media with a lattice constant comparable to the wavelength [5]. Also, negative refraction of microwaves in a metallic photonic crystal prism whose spectral response manifests both positive and negative refraction has been demonstrated [6].

The suitability of obtaining NRI materials at optical frequencies has been shown by using a pair of sub-wavelength hole arrays drilled into very thin metallic plates [7, 8], losses still being a serious drawback because the designs were not optimized under the extraordinary optical transmission (EOT) [9] criterion. These results have been further expanded in the millimetre wave range where losses due to conductors are much lower [10]. However, what is really relevant is that in this last work, the NRI behaviour of such stacks has been successfully linked to the concept of EOT, which is the subject of this work. Furthermore, alternative theoretical work analysing the key relationship between both phenomena has been recently reported [11]. An additional reduction of losses can be achieved with an original design of a double periodicity in the sub-wavelength hole arrays that increases the density of holes [12].

Here, we present a direct pure geometrical and experimental demonstration of effective one-dimensional negative refraction at millimetre waves in a prism made of stacked sub-wavelength metallic hole arrays sandwiched in air, with low losses. We study in detail the conditions to

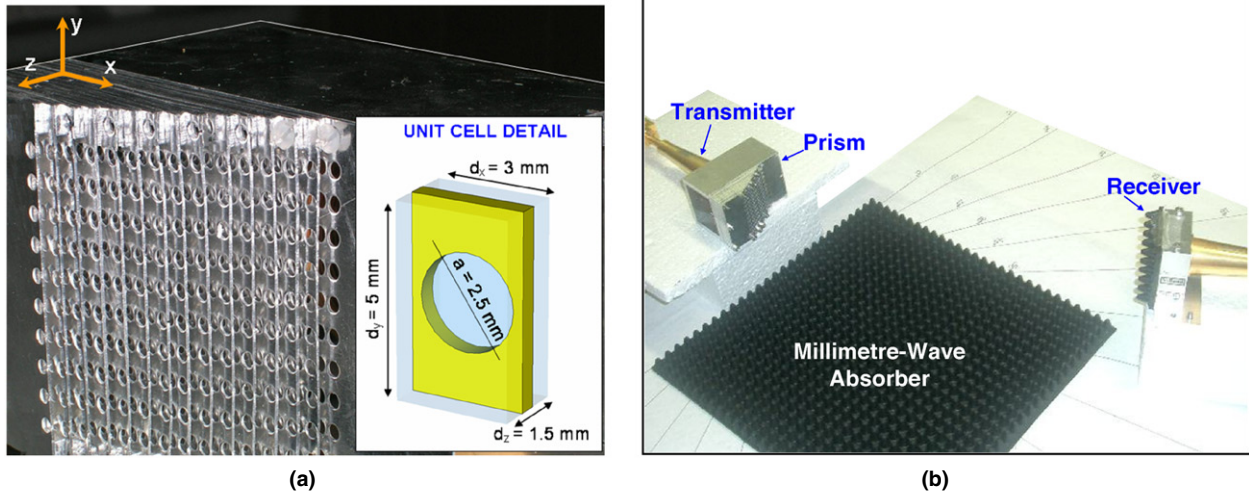


**Figure 1.** (a) Fabricated prism with the following parameters: hole diameter  $a = 2.5$  mm,  $d_x = 3$  mm,  $d_y = 5$  mm and  $d_z = 1.5$  mm, the angle of the prism is  $26.6^\circ$ ; (inset) unit cell dimensions. (b) Photograph of the experimental set-up showing the prism illuminated with the transmitter horn antenna (located on the top left side) and the receiver horn antenna on the right. The floor is covered with a piece of millimetre-wave absorbing material to minimize extraneous components due to reflection.

get negative refraction, analysing three different cases with numerical simulations and experiments: structure excited at the extraordinary transmission resonance, behaviour at the next band and excitation with the orthogonal polarization. Out of these, only the first case has been published previously [13] and by extending the study to other polarizations and bands, we show that negative refraction is only achieved in the first case. Moreover, measurements are done in the near field zone and thus we add further light to the results reported in [13] and to the recent work at optical wavelengths following our double periodicity dielectric embedding approach [14].

## 2. Design and simulation results

The proposed structure consists of several stacked sub-wavelength hole arrays perforated in an aluminium plate with hole diameter  $a = 2.5$  mm, cut-off frequency at 70 GHz, transversal periodicities,  $d_x = 3$  mm and  $d_y = 5$  mm, and metal thickness  $w = 0.5$  mm. In this case, ET appears near 57 GHz, contrasting with the fact that the cut-off frequency of each hole is 70 GHz. Along the longitudinal dimension, the period between the hole array plates is  $d_z = 1.5$  mm. Finally, in order to obtain the prism, one needs to remove the number of periods step by step along the  $x$  dimension; see the photograph of the prototype in figure 1(a).

By using the eigenmode solver of CST Microwave Studio™ we have computed the one-dimensional dispersion diagrams of the structure described previously; see figure 2. It should be noted that only this 1D dispersion diagram and not the 2D representation is required for the analysis of this wedge experiment since the refraction is actually caused by the negative phase difference acquired by adjacent holes of the stepped output face [15]. To this end, a unit cell is taken and periodic boundary conditions are applied with a specific phase shift across the cell in the longitudinal dimension, i.e. the stack direction, whereas in the cross-sectional dimensions electric and magnetic walls are used. For vertical polarization

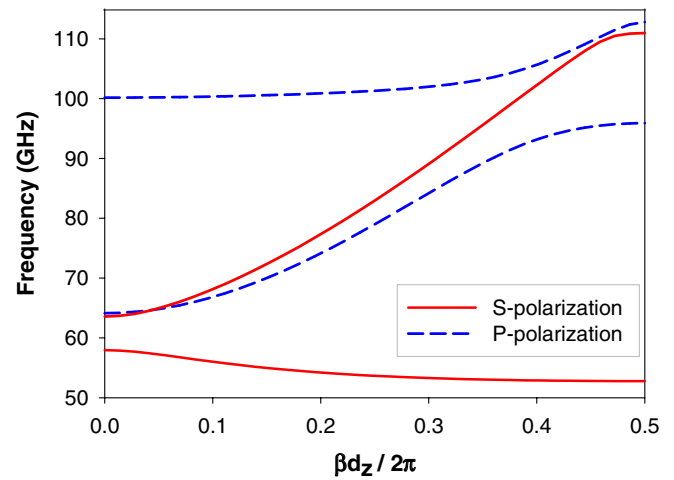


**Figure 2.** Dispersion diagram showing the first couple of bands for s- (solid red) and p- (dashed blue) polarizations.

(or s-polarization, i.e. electric field along  $y$ ) the top and bottom faces are electric walls, whereas the lateral faces have magnetic walls as boundary conditions. On the other hand, for horizontal polarization illumination (p-polarization, i.e. electric field along  $x$ ), the transversal boundary conditions interchange their roles. The electromagnetic wave propagating in this artificial waveguide thus resembles the one of a TEM plane wave propagating along  $z$  [16].

The first band of the stacked sub-wavelength hole array structure under vertical polarization (s-polarization) appears near the EOT frequency with a clear negative slope, i.e. phase velocity opposite to the group velocity. This fact suggests the suitability of designing a prism for a direct demonstration of the existence of negative refraction. On the other hand, for the orthogonal polarization the first band is located between 64 and 96 GHz and is clearly right-handed (RH). Note that with this polarization and due to the double periodicity of the hole array, EOT resonance is not excited. With regard to the second

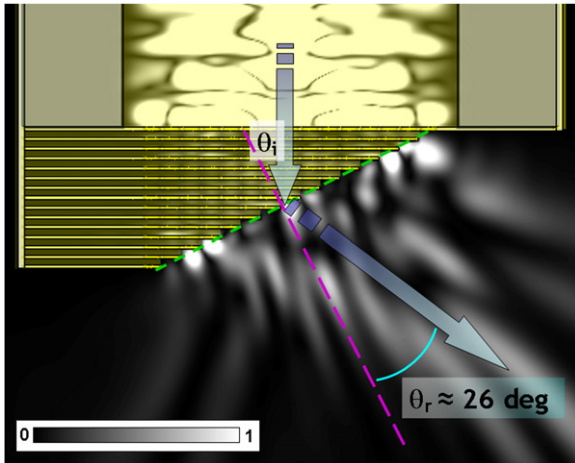


**Figure 3.** Full-wave simulation of the power density evolution in the near field zone of the prism at 53.5 GHz where an index of refraction  $n = -1$  is expected.

s-polarization band, it extends from 63.6 to 111 GHz and also has a RH character.

Using the mentioned software, we compute the evolution of the power flow in the proposed prism of figure 1 along the  $x$ - $z$  cutting plane (i.e. the plane in which the radiation pattern is recorded in the subsequent experiment) at a frequency of 53.5 GHz. At this frequency the expected index of refraction is  $n = -1$ , as it can be qualitatively inferred from the direction of the major beams of figure 3 (see also [13], where the direction of the power flow is highlighted by electric field wavefronts). Note that the power flow emerges breaking the usual direction of Snell's law as can be expected in a NRI metamaterial, and the transmitted angle is  $-26^\circ$ .

### 3. Experimental results and discussion

The prototype was fabricated in aluminium; see figure 1(a). The angular evolution of the received radiated power was measured using an AB Millimetre™ Quasioptical Vector Network Analyzer placing the receiver at 100 mm in the near field zone of the prism structure with a frequency span of 45–75 GHz. The measurement is done on the  $x$ - $z$  plane exciting the prism with the two orthogonal polarization states mentioned in the previous section. The Gaussian beam source and the sensor are two identical corrugated horn antennas attached by coaxial cables to the analyzer. A photograph of the experimental set-up is shown in figure 1(b).

At the experimental distance of the receiver (100 mm) one can assume operation inside the near field zone where it is expected to have a well-collimated beam. This can be checked by using the confocal parameter (also called the Rayleigh range) defined as  $z_c = \pi w_0^2 / \lambda$  [17],  $w_0$  being the beam waist and  $\lambda$  the wavelength. Taking  $w_0 = 60$  mm (the aperture side) gives  $z_c = 2261$  mm, proving our near field operation hypothesis.

In figure 4(a), the received power as a function of the frequency and the deflection angle when the electric field is polarized along the large hole periodicity (s-polarization) is presented. It can be seen that for the first frequency band

(from 51 to 60 GHz), the radiation pattern emerges with a negative angle relative to the normal, in good agreement with the calculated dispersion diagram. This demonstrates unambiguously that the proposed prism presents a negative index of refraction.

Concerning losses, it should be noted that they are around  $-10$  dB, but this feature could be improved by designing a matched feed to the prism since the current design is based on corrugated horn illuminating a parallel plate waveguide terminated in the structure, without taking care of matching optimization. This demonstrates the suitability of this design for achieving low-loss negative refraction devices.

Moreover, as the frequency increases, the maximal values of figure 4(a) approach the normal, demonstrating the dispersion of the index of refraction, i.e. it is a function of frequency. There, the index comes close to a value  $n \approx 0$  but still remains negative as derived from Snell's refraction law. This phenomenon can be very useful for the design of innovative antennas. Also note the presence of Wood's anomaly at 60 GHz and the appearance of the second band at 64 GHz with a positive refraction characteristic, in good agreement with the computed diagram.

In figure 4(b) a similar diagram is shown corresponding to the p-polarization measurement. In this case a single RH band starting at 63 GHz is observed within the frequency span, in accordance with the dispersion diagram.

The simulation and experimental results shown previously show that the prism presents negative refraction only at the EOT resonance. This can be clarified using an engineering-based lumped element model. As explained in [10], a hole operating below the cut-off has an inductive behaviour. EOT resonance leads to total transmission through sub-wavelength inductive holes and thus the perforated plate can be modelled as a shunt inductance. Besides, by stacking several EOT plates, a series capacitance appears due to the electric coupling between plates. Both lumped elements define an inverse transmission line that supports backward waves.

For the orthogonal polarization, the large hole density axis is parallel to the electric field and EOT resonance is not excited. This case is comparable to a classical perforated plate frequency selective surface [17], where the structure operates as a close-packed waveguide array. This kind of structure presents a pass-band characteristic starting at a frequency slightly below the hole cut-off and extending up to the Wood's anomaly. Therefore, the holes operate fundamentally above the cut-off and consequently each plate cannot be modelled as a shunt inductance but rather as a shunt capacitance. As in the previous case, the periodic stack introduces a series capacitance resulting in a completely different shunt-series capacitance model.

Finally, the second s-polarization band case is very similar to the previous one, since now the holes operate above the cut-off. The same circuit model with different numerical values can be applied in this case. Concentrating now on the second p-polarization band, see figures 2 and 4(b), it is observed that it starts at 100 GHz, which is exactly the Rayleigh–Wood anomaly frequency corresponding to the period along  $x$ . Observing carefully the dispersion diagram, it is evident that

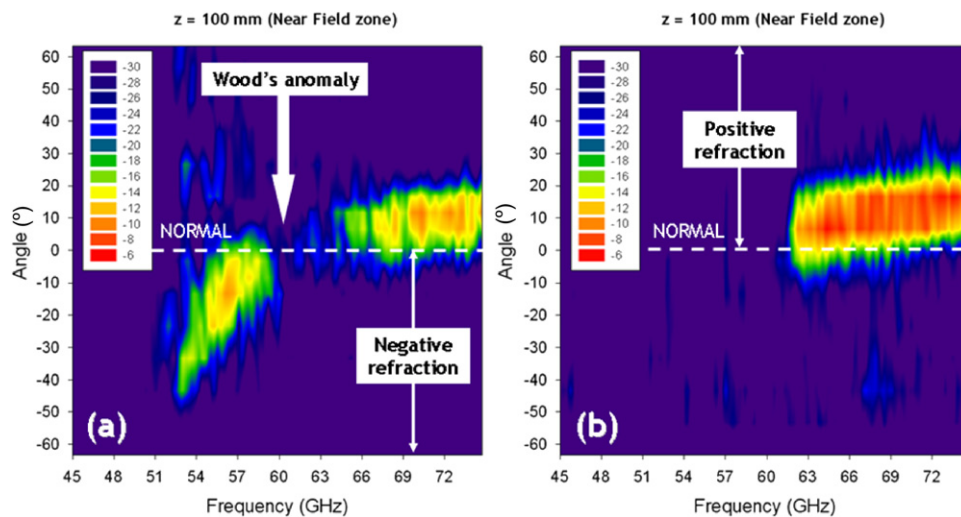


**Figure 4.** Measured received power distribution on the  $x$ - $z$  cutting plane in the near field zone (100 mm) recorded as a function of the angle and the frequency. (a) s-polarization excitation and (b) p-polarization excitation.

the Wood's anomaly introduces a band-gap that breaks the bands modifying the picture compared with the second s-polarization band.

#### 4. Conclusions

By stacking sub-wavelength hole arrays, left-handed metamaterials have already been achieved for frequencies in the microwave and millimetre wave range with the aimed low losses property due to its intrinsic enhanced transmission phenomenon caused by the sub-wavelength hole arrays. The small holes also provide the necessary shunt inductance to cause left-handed propagation in an inverse transmission line that has series capacity when the plates are close enough.

Negative refraction has been demonstrated with a prism constructed by stacking the mentioned hole arrays, and the dispersive behaviour has been experimentally shown. Furthermore, the given results have been measured in the near field where a well-collimated beam can be assumed. It has been shown that EOT is essential in order to achieve negative refraction. Besides, a discussion about the origin of the second band and also of the p-polarization bands has been presented.

The experimental results obtained in this prism can be applied for the design of novel practical devices like (de)multiplexer [18], antennas and frequency selective surfaces in any frequency range.

#### Acknowledgments

This work has been financially supported by the Spanish Government under contract Consolider 'Engineering Metamaterials' CSD2008-00066.

#### References

- [1] Klar T A, Kildishev A V, Drachev V P and Shalaev V M 2006 *IEEE J. Selected Top. Quantum Electron.* **12** 1106
- [2] Pendry J B 2000 *Phys. Rev. Lett.* **85** 3966
- [3] Shelby R A, Smith D R and Schultz S 2001 *Science* **292** 77
- [4] Veselago V G 1968 *Sov. Phys.—Usp.* **10** 509
- [5] Kosaka H, Kawashima T, Tomita A, Notomi M, Tamamura T, Sato T and Kawakami S 1998 *Phys. Rev. B* **58** 10096
- [6] Parimi P V, Lu W T, Vodo P, Sokoloff J, Derov J S and Sridhar S 2004 *Phys. Rev. Lett.* **92** 127401
- [7] Zhang S, Fan W, Panoiu N C, Malloy K J, Osgood R M and Brueck S R J 2005 *Phys. Rev. Lett.* **95** 137404
- [8] Dolling G, Enkrich C, Wegener M, Soukoulis C M and Linden S 2006 *Science* **312** 892
- [9] Ebbesen T W, Lezec H J, Ghaemi H, Thio T and Wolf P A 1998 *Nature* **391** 667
- [10] Beruete M, Sorolla M and Campillo I 2006 *Opt. Express* **14** 5445
- [11] Mary A, Rodrigo S G, García-Vidal F J and Martín-Moreno L 2008 *Phys. Rev. Lett.* **101** 103902
- [12] Beruete M, Sorolla M, Navarro-Cía M, Falcone F, Campillo I and Lomakin V 2007 *Opt. Express* **15** 1107
- [13] Navarro-Cía M, Beruete M, Sorolla M and Campillo I 2008 *Opt. Express* **16** 560
- [14] Valentine J, Zhang S, Zentgraf T, Ulin-Avila E, Genov D A, Bartal G and Zhang X 2008 *Nature* **455** 376
- [15] Beruete M, Navarro-Cía M, Sorolla M and Campillo I 2009 *Phys. Rev. B* **79** 195107
- [16] Beruete M, Campillo I, Navarro-Cía M, Falcone F and Sorolla Ayza M 2007 *IEEE Trans. Antennas Propag.* **55** 1514
- [17] Goldsmith P F 1998 *Quasioptical Systems—Gaussian Beam, Quasioptical Propagation and Applications.* (Piscataway, NJ: IEEE)
- [18] Navarro-Cía M, Beruete M, Campillo I and Sorolla M 2009 *IEEE Antennas Wireless Propag. Lett.* **8** 212